

Synthesis, X-ray Crystal Structures, Stabilities, and in Vitro Cytotoxic Activities of New Heteroarylacrylonitriles

Franciszek Sączewski,^{*,†} Przemysław Reszka,^{†,‡} Maria Gdaniec,[§] Renate Grünert,[‡] and Patrick J. Bednarski^{*,‡}

Department of Chemical Technology of Drugs, Medical University of Gdańsk, Al. Gen. Hallera 107, 80-416 Gdańsk, Poland, Department of Pharmaceutical and Medicinal Chemistry, Institute of Pharmacy, University of Greifswald, F.-L.-Jahn Strasse 17, 17489 Greifswald, Germany, and Faculty of Chemistry, A. Mickiewicz University, 60-780 Poznań, Poland

Received November 14, 2003

Twenty-three acrylonitriles, substituted at position 2 with either triazoles or benzimidazoles and at position 3 with various substituted furan, thiophene, or phenyl rings, were prepared by Knoevenagel condensation and tested for in vitro cytotoxic potency on 11 human cancer cell lines. X-ray crystal analysis of two representative compounds showed that the olfenic bond is *E*-configured. Structure–activity–relationships (SAR) indicated that position 2 is flexible for substituents with various nitrogen heterocyclics while position 3 is very sensitive to change; the most potent compounds contained a 5-nitrothiophen-2-yl ring at position 3 and either benzimidazol-2-yl (**11**) or a 5-benzyl-1*H*-[1,2,4]-triazol-3-yl (**7**) group at position 2 of acrylonitrile. SARs for the thiophen-2-yl-benzimidazoles show the following trend for position 5: NO₂ ≫ H > Cl = CH₃. Compound **11** was on average 10- and 3-fold more potent than cisplatin and etoposide, respectively. However, the acrylonitrile functionality is not an absolute requirement for cytotoxic activity because replacement of the nitrile group for either a hydrogen or a methyl group also gave active compounds. The acrylonitriles caused delayed cell death characterized by giant cells with multilobed nuclei. Compound **11** was found to bring about the increase in the activities of caspases 3 and 9 in the HL-60 cell line in a manner similar to etoposide, strongly indicating that apoptosis is the mechanism of cell death. The selectivity of various compounds toward cancer cells was estimated by comparing the IC₅₀ values obtained from a noncancerous epithelial cell line, h-TERT-RPE1, with the average IC₅₀ value from the cancer cell lines; **11** showed an average 1.7-fold greater activity toward cancer cells. The stabilities of the new compounds under cell culture conditions, estimated by HPLC, indicated that a major fraction of the compounds were lost from the medium over the first 24 h.

Introduction

2,3-Disubstituted acrylonitriles represent an interesting class of biologically active compounds. These compounds have been shown to possess spasmolytic,¹ estrogenic,² hypotensive,³ antioxidative,⁴ tuberculostatic,⁵ antitrichomonal,⁶ insecticidal,⁷ and cytotoxic⁸ activities. Of particular interest are derivatives substituted in position 2 with triazines and in position 3 with nitro-furan (Table 1); such compounds have recently been found to possess potent cancer cell growth inhibitor activity in the National Cancer Institute 60 cell line screen.⁹

To explore the structure–activity–relationships of this class of compounds in more detail, analogues have been prepared with variations at both positions 2 and 3 of the acrylonitrile moiety. By replacement of the triazine ring for either 1,2,4-triazole or benzimidazole ring systems, the importance of this position (i.e., ring A) on the cytotoxic activity has been studied. At position 3 (i.e., ring B), derivatives with various substituted benzene,

furan, or thiophene rings have been synthesized (Table 1). To investigate the importance of the cyano group on the cytotoxic activity, analogues lacking this group have also been prepared. Herein, the testing of the new series of acrylonitriles for cell growth inhibition on a panel of 11 human cancer cell lines is reported. The mechanism of cell death has also been investigated by monitoring the time-dependent activities of the apoptotic enzymes caspases 3 and 9. To gain information on the selectivity toward cancer cells, cytotoxicity has also been assessed on a noncancerous, immortalized human epithelial cell line, h-TERT-RPE1. In addition, the stabilities of selected compounds under cell culture conditions have been investigated.

Chemistry

Synthesis. In our investigations we synthesized two series of acrylonitrile derivatives: series A (compounds **1–9**, Table 1) characterized by the presence of 1,2,4-triazole as ring A and various aryl/heteroaryl substituents as ring B; series B containing benzimidazole as ring A and aromatic or heteroaromatic rings as ring B (compounds **10–26**, Table 1).

The desired acrylonitriles **1–9** were prepared by the Knoevenagel condensation reaction of the corresponding (1,2,4-triazol-3-yl)acetonitriles with aldehydes, typically

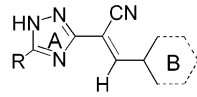
* To whom correspondence should be addressed. For F.S.: e-mail, saczew@farmacja.amg.gda.pl; phone, (+48) 58 3493250; fax, (+48) 58 3493257. For P.J.B.: e-mail, bednarsk@pharmazie.uni-greifswald.de; phone, (+49) 3834 864883; fax, (+49) 3834 864874.

[†] Medical University of Gdańsk.

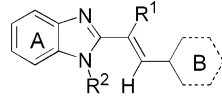
[‡] University of Greifswald.

[§] A. Mickiewicz University.

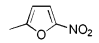
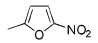
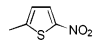
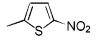
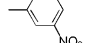
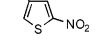
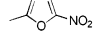
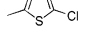
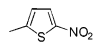
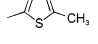
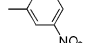
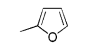
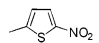
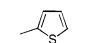
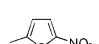
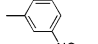
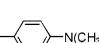
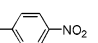
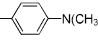
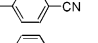
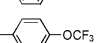
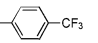
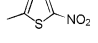
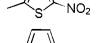


Table 1. Structures of Acrylonitrile Derivatives 1–26



Series A



Series B

Series A				Series B				
No	R	Ring B	Method	No	R ¹	R ²	Ring B	Method
1	CH ₃		A	10	CN	H		B
2	CH ₃		A	11	CN	H		B
3	CH ₃		A	12	CN	H		B
4	C ₆ H ₅		A	13	CN	H		B
5	C ₆ H ₅		A	14	CN	H		B
6	C ₆ H ₅		A	15	CN	H		B
7	C ₆ H ₅ CH ₂		A	16	CN	H		B
8	C ₆ H ₅ CH ₂		A	17	CN	H		B
9	C ₆ H ₅ CH ₂		A	18	CN	H		B
				19	CN	H		B
				20	CN	H		B
				21	CN	H		B
				22	CN	H		B
				23	CN	H		B
				24	H	COCH ₃		C
				25	H	H		D
				26	CH ₃	H		C

in the presence of piperidine in ethanol at reflux (Table 1, method A).

Analogous condensation of 2-cyanomethylbenzimidazole with aromatic aldehydes was performed in the presence of KOH in ethanol at room temperature, giving rise to the formation of products **10**–**23** (Table 1, method B).

To determine whether simpler, readily available compounds lacking the cyano group would retain any of the activity of the parent compound **11**, the benzimidazole derivatives **25** and **26** (R¹ = H, CH₃) were synthesized by condensation of 2-methyl- and 2-ethylbenzimidazole, respectively, with 5-nitrothiophene-2-aldehyde in acetic anhydride under reflux (Table 1, method C). In the case of 2-methylbenzimidazole, however, this reaction led to the formation of *N*-acetyl derivative **24**, which proved to be rather unstable in aqueous solution and partially hydrolyzed to the compound **25**, rendering this compound unsuitable for biological testing.

The deacetylated benzimidazole **25** could be obtained in pure form according to the method described previously by Prousek¹⁰ by using a multistep procedure based on the Wittig reaction (see Experimental Section, Table 1, method D). The coupling constants in the ¹H NMR spectrum (*J* = 15.5 Hz) provide evidence that the stereochemistry of the olefinic bond is *trans*.

Crystal Structure Analyses. The configuration of the acrylonitrile double bond could not be established by NMR methods; thus, X-ray crystallographic investigations were performed. X-ray crystal structures of compounds **3** and **24** are shown in Figures 1 and 2, respectively. These structures establish that the olefinic bond is *E*-configured.

There is strong conjugation between the different moieties constituting the skeleton of molecules **3** and **24**. Because of this effect, the aromatic rings in **3** and **24** are only twisted slightly relative to the central vinyl group.

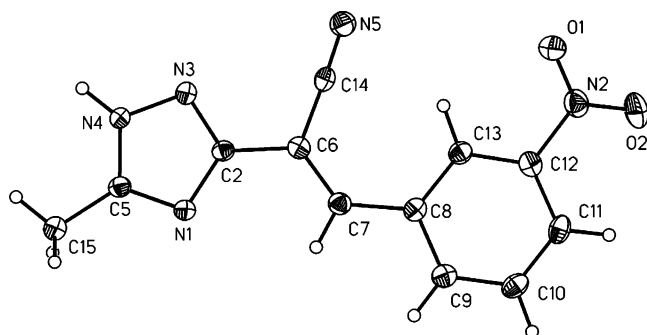


Figure 1. ORTEP drawing of **3** with the atom labeling scheme. Ellipsoids are drawn at the 50% probability level.

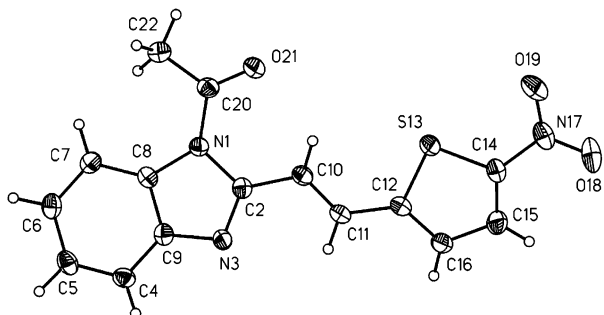


Figure 2. ORTEP drawing of **24** with the atom labeling scheme. Ellipsoids are drawn at the 50% probability level.

In **3** the torsion angles about the partially double C–C bonds to the 1,2,4-triazole and phenyl rings are $-14.7(3)^\circ$ and $15.3(3)^\circ$, respectively, and the dihedral angle between the two aromatic moieties is $2.61(7)^\circ$. The vinyl group, bearing three conjugated substituents, has the double bond length of $1.349(2)$ Å, significantly longer than those of the disubstituted vinyl groups in 2-styrylbenzimidazoles and 2-styrylimidazoles (1.304 – 1.332 Å).¹¹

In **24** the thiophenyl ring is approximately coplanar with the vinyl group. The steric interaction of the vinyl and acetyl groups results in a twist of $22.1(3)^\circ$ of the benzimidazole moiety relative to the vinyl group and a twist of $16.1(1)^\circ$ between the acetyl group and the benzimidazole ring; in effect, the vinyl H10 atom and acetyl O21 are $2.23(2)$ Å apart. Bond distances and bond angles in **24** are within normal ranges (Tables 1S–14S).

Molecular Modeling. As evidenced from both X-ray crystallographic studies and ¹H NMR spectroscopic data (see Experimental Section), the olefinic bond in the compounds of series A and B adopted the *E* configuration. However, owing to the different orientations of the heterocyclic rings, these compounds can exist in the form of four low-energy conformers. Literature reports for similar compounds suggest that such conformers might be stable on an NMR time scale.¹² We have therefore determined the preferred conformation of the most active compound **11** by computation of the internal energies for the rotamers **11A–D** (Figure 3) with an ab initio quantum mechanics Hartree–Fock method.¹³ Analysis of the energy differences (Table 2) clearly indicates that the most stable are rotamers **11A** and **11B**, which differ in energy by 0.1 kcal/mol. Moreover, the conformational analysis around the C β –thiophene bond performed at 10° increments revealed that both of these rotamers can adopt the out-of-the-plane conformation at a low-energy cost of 1.5 kcal/mol.

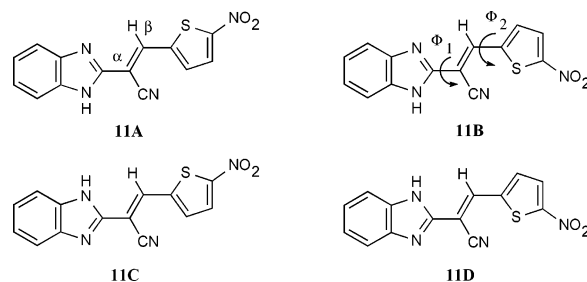


Figure 3. Possible conformations of **11**.

Table 2. Conformational Search on Compound **11**

conformer	Φ_1 [deg]	Φ_2 [deg]	E [au]	ΔE^a [kcal/mol]	dipole moment [D]
11A	-0.2	-0.2	-1 299.717 263 2	0.1	5.63
11B	-0.5	-1.9	-1 299.717 424 4	0.0	4.93
11C	-22.2	-3.3	-1 299.709 556 0	4.9	5.38
11D	-23.7	-1.9	-1 299.707 959 3	5.9	9.78

^a Energy of each conformer after minimization, relative to the global minimum.

Table 3. Primary Screen of All 26 Compounds at $20 \mu\text{M}^a$

compd	LCLC-			compd	SISO	5637	KYSE-70
	SISO	103H	KYSE-510				
1	-8.7	-8.4	-21.3	15	106.1	86.1	56.6
2	-8.8	-8.4	-21.3	16	82.4	49.3	30.8
3	98.1	68.8	94.1	17	54.2	14.4	55.4
4	-7.9	-8.4	-20.9	18	99.2	73.9	88.0
5	-9.9	-6.5	-21.7	19	95.0	61.1	124.4
6	85.5	56.4	108.0	20	99.2	75.6	99.3
7	-8.7	-8.4	-21.3	21	72.1	64.9	75.8
8	-8.1	-7.3	-20.7	22	71.7	66.0	96.7
9	1.2	-1.8	-1.01	23	61.8	34.4	69.7
10	-8.2	-8.0	-21.2	25	-1.8	0	0.7
11	18.0	-6.5	20.5	26	-1.3	0.5	2.4
12	82.3	8.6	nd	12	82.3	80.0	nd
13	102.2	13.4	nd	13	102.2	44.6	nd
14	64.5	5.9	nd	14	64.5	47.8	nd

^a Results are the average percent growth values from eight determinations in a single experiment. Italic compound numbers indicate those that were evaluated further in the secondary screen.

Biology

Cytotoxicity Testing. Primary screening of the new compounds for cytotoxic activity took place on three cell lines (Table 3). Compounds that showed enough activity at $20 \mu\text{M}$ to give percent growth values of less than 50% in one or more of the cell lines were investigated further.

Secondary screening to determine potency was performed on a panel of 11 human cancer cell lines: a cervical cancer, SISO; a non-small-cell lung cancer, LCLC-103H; three esophagus cell lines, KYSE-70, -510, and -520; three bladder cell lines, RT-4, RT-112, and 5637; two pancreas lines, YAPC and DAN-G; and the breast cancer cell line, MCF-7. Figure 4 shows representative dose–response curves for compound **11** and cisplatin in the YAPC and DAN-G cell lines. Table 4 lists the IC_{50} values calculated from the dose–response data and reports the average IC_{50} value and the relative standard deviation for the tested cell lines.

The most active compounds possess at position 3 of the acrylonitrile functionality a 5-nitrothiophene ring and at position 2 benzimidazole (**11**), 5-benzyltriazole (**7**), or 5-methyltriazole (**2**) heterocycles. Interestingly, the presence of methyl, phenyl, or benzyl substituents in position 5 of the triazole ring leads to compounds with good potency (e.g., **2**, **5**, **7**), suggesting that this position

Table 4. IC₅₀ (μM) Values in 11 Human Cancer Cell Lines and a Human Epithelial Cell Line (h-TERT-RPE1)^a

compd	mean ^b	RSD (%) ^c	RT-4	RT-112	5637	KYSE-70	KYSE-510	KYSE-520	YAPC	DAN-G	SISO	LCLC-103H	MCF-7	h-TERT-RPE1
11	0.23	40	0.27	0.36	0.15	0.16	0.33	0.11	0.16	0.32	0.31	0.17	0.16	0.39
7	0.47	33	0.59	0.65	0.32	0.42	0.53	0.29	0.36	0.50	0.78	0.31	0.42	0.51
2	0.51	36	0.90	0.67	0.22	0.44	0.56	0.60	0.41	0.57	0.51	0.33	0.38	0.69
25	0.57	31	0.89	nd	0.27	nd	nd	nd	nd	nd	nd	0.56	nd	0.21
8	0.59	51	1.37	0.75	0.40	0.40	0.62	0.75	0.45	0.49	0.37	0.29	0.61	0.42
10	0.60	31	0.99	0.69	0.48	0.45	0.75	0.62	0.57	0.69	0.33	0.41	0.65	0.60
5	0.61	37	1.03	0.83	0.48	0.35	0.63	0.57	0.32	0.42	0.89	0.54	0.68	0.42
1	0.85	46	1.48	1.00	0.54	0.66	0.90	0.86	0.85	1.00	0.27	0.35	1.47	0.69
4	1.38	31	1.85	1.51	1.22	1.17	1.35	1.62	1.40	1.52	1.20	0.70	1.62	1.16
9	3.06	46	2.50	3.69	1.38	2.53	3.36	6.26	3.48	4.11	3.24	1.65	1.49	nd
26	3.41	44	4.67	nd	3.65	5.11	nd	nd	nd	3.73	3.28	0.44	2.97	nd
23	12.36	45	16.33	nd	12.19	15.64	nd	nd	nd	17.61	14.03	1.60	9.11	nd
16	13.8	54	14.59	nd	17.83	8.78	nd	nd	nd	14.99	25.86	2.50	11.23	nd
17	15.67	61	7.68	nd	15.24	22.53	nd	nd	nd	15.83	30.89	1.13	16.39	nd
14			>20	nd	20.05	nd	nd	nd	nd	>20	>20	2.11	nd	nd
13			>20	nd	22.42	nd	nd	nd	nd	>20	>20	1.97	nd	nd
12			>20	nd	>20	nd	nd	nd	nd	>20	>20	1.42	nd	>5
cisplatin	2.14	91	3.70	2.14	0.31	1.49	0.88	5.07	6.03	1.39	0.20	1.63	0.74	3.04
etoposide	0.64	65	1.33	0.22	0.53	0.79	0.70	0.41	1.32	0.38	0.15	nd	0.54	0.09

^a Values are averages of two to three independent determinations. Individual values did not differ by more than 20%. nd: not determined.

^b Averaged IC₅₀ values over all tested cancer cell lines. ^c Relative standard deviation.

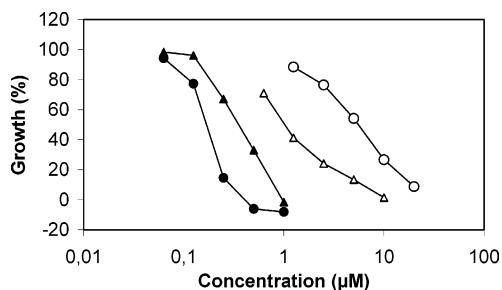


Figure 4. Representative dose–response curves for **11** (solid symbols) and cisplatin (open symbols) in the YAPC (circles) and DAN-G (triangles) human pancreas cell lines.

is not critical and thus is free for variations. Compared to cisplatin, compound **11** is on average 10-fold more potent and in some cell lines (i.e., KYSE-520 and YAPC) even 50-fold more potent (Table 4).

Interestingly, when the 5-nitrothiophen ring is substituted to the acrylonitrile functionality at position 3 instead of at position 2 of the thiophene ring, activity is almost completely lost (compare the isomers **11** with **12** in Table 3). Replacement of the 5-nitro group for either chloro (**13**), methyl (**14**), or hydrogen (**16**) results in severe reductions in activity (Table 4), with the average order of **11** >> **16** > **13** = **14**. Replacement of the thiophene for a furan ring reduces the average potency (compare **1** with **2**, **4** with **5**, and **10** with **11**), but on a few occasions the furan and thiophene analogues showed equivalent activity, e.g., for **10** and **11** in the SISO cell line. Compounds with 3-substituted benzene rings were the least active. Compound **18**, which possesses a 4-nitrobenzene ring as a 5-nitrothiophene isostere, was inactive. On the other hand, the 3-nitrobenzene isomer **17** showed weak activity.

Not all active compounds had at position 3 of the acrylonitrile moiety aromatic rings substituted with nitro groups; two exceptions were the 4-dimethylaminophenyl triazole (**9**) and on the 4-trifluoromethylphenylbenzimidazole (**23**), but these compounds were only weakly active (Table 4). Although the cyano group of the acrylonitrile moiety was not an absolute requirement for activity, compounds lacking this group (i.e., **25** and **26**) were less active compared to their acryloni-

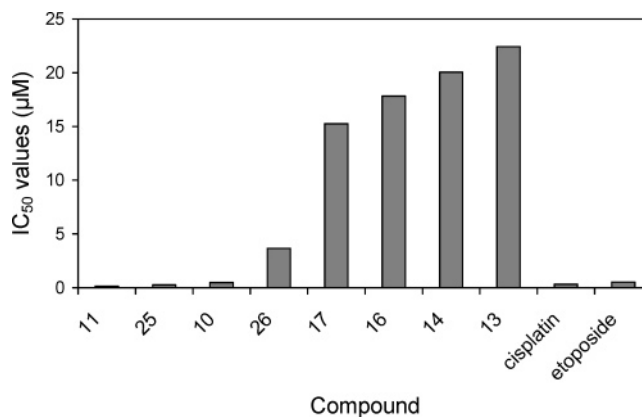


Figure 5. Representative SAR of some benzimidazole derivatives in the 5637 cell line. IC₅₀ values are the averages of two separate determinations whereby the individual values did not differ by more than 20%.

trile counterpart **11**. Interestingly, replacement of the nitrile group for hydrogen (compare **11** with **25**) had less of an effect than replacement for a methyl group (compare **11** with **26**). Representative SAR of the benzimidazole derivatives in the 5637 cell line are summarized in Figure 5.

To establish the selectivity toward cancer cells, testing of the more potent compounds on the noncancerous human epithelial cell line h-TERT-RPE1 was done. This immortalized cell line is derived from human corneal epithelium transfected with human telomerase reverse transcriptase (hTERT).¹⁴ As evidenced in Table 4, the potencies of the compounds were roughly the same in the h-TERT-RPE1 cells and in the average human cancer cell line, indicating little selectivity toward cancer cells in general. Nevertheless, when individual cell lines such as 5637, KYSE-70, LCLC-103H, and MCF-7 are compared with h-TERT-RPE1, then a modest degree of selectivity for compounds **2** and **11** became apparent. It was found that known antitumor agents such as cisplatin and etoposide are also nonselective toward cancer cells; in fact, the h-TERT-RPE1 cell line was the most sensitive of the cell lines tested to the growth inhibitory action of etoposide (Table 4).

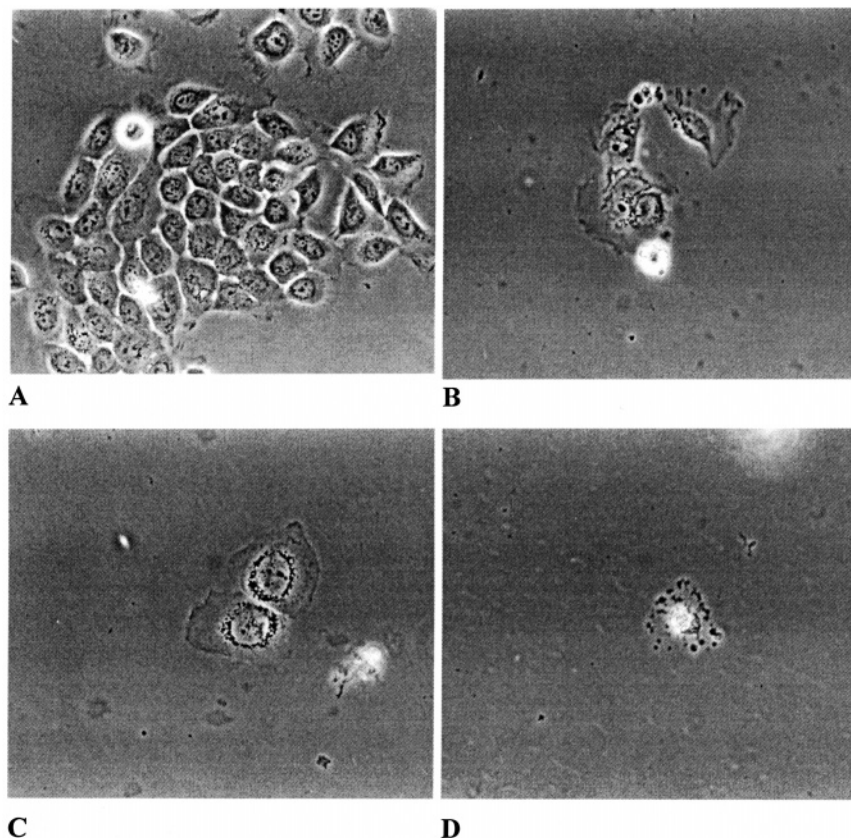


Figure 6. Cell line 5637 treated for 96 h with various substances: (A) control cells; (B) 1.0 μM **8**; (C) 0.5 μM **11**; (D) 1.0 μM **7**. All pictures are at 400-fold magnification.

Mechanism of Cell Death. Morphological changes in the cells as a result of treatment with representative acrylonitriles were documented by photography. In Figures 6–8 the effects of compounds **7**, **8**, and **11** on the appearance of the 5637, LCLC-103H, and SISO cells are compared with nontreated controls. These changes first became apparent 3–4 days after treatment. The presence of giant cells with large, often multilobed nucleus (Figures 6B,C, 7C,D, and 8C) is characteristic, in particular for **11**. Also, cells with clear vacuoles in the cytoplasm (Figure 8D) or absence of a defined nucleus (Figure 8B) were observed. Occasionally, very small cells (Figure 7B) or cells lacking a cell membrane (Figure 6D) were found.

These results prompted us to investigate in more detail the mechanism of cell death caused by the most potent compound **11**. Antitumor agents are known to induce cancer cell death by a mechanism of apoptosis, characterized by the release of cytochrome *c* from the mitochondria, the induction of various caspase enzymes, condensation of the chromosomes, and the fragmentation of nuclear DNA.¹⁵ For example, the widely used antitumor agent etoposide is known to cause induction of caspase 3 and 9 activities in HL-60 human leukemia cells within hours of exposure to the drug.¹⁶ An assay based on the HPLC detection of fluorescent products from specific caspase 3 and 9 substrates was developed to specifically monitor the time-dependent activities of these two caspases in cultures of HL-60 cells. To validate the assay, the increases in the two caspase activities caused by etoposide were monitored and found to follow a similar time frame as previously reported (Figure 9).¹⁶ Figure 9 shows that at a cytotoxic concen-

tration (50 μM), compound **11** causes a very similar induction pattern of both enzymes, strongly indicating that this compound is killing cells by a mechanism of apoptosis.

Stability Studies

A number of chemical reactions are imaginable for acrylonitriles under the conditions of the cytotoxicity assays, e.g., Michael addition of thiols, retro-Knoevenagel reactions, nitro group reductions. Such reactions may play a role in the mechanism of action and could influence the pharmacokinetics of the substances. Thus, the stability of selected compounds in cell culture was investigated. Two methods were chosen for assessing compound stability under cell culture conditions: (1) a time-dependent cytotoxicity assay; (2) time-dependent RP-HPLC assay.

The cytotoxic potency of a substance will increase with the duration of drug exposure if the compound concentrations remain at cytotoxic levels during the drug exposure.¹⁷ Figure 10 shows the respective time-dependent dose–response curves for **7** on the 5637 cell lines. Cells were treated either continuously for 96 h with substance or 24, 48, and 72 h, after which time the medium was replaced with fresh medium and incubation continued to 96 h. With increasing duration of exposure, no changes in growth inhibitory potency were observed; i.e., **7** had reached maximal activity by 24 h. Also, for compounds **10** and **11** no changes in the IC_{50} values were observed after 24 h (data not shown). This can be interpreted that these acrylonitriles are not stable in culture, and by 24 h most of the compound has been inactivated. However, for compound **9**, the IC_{50}

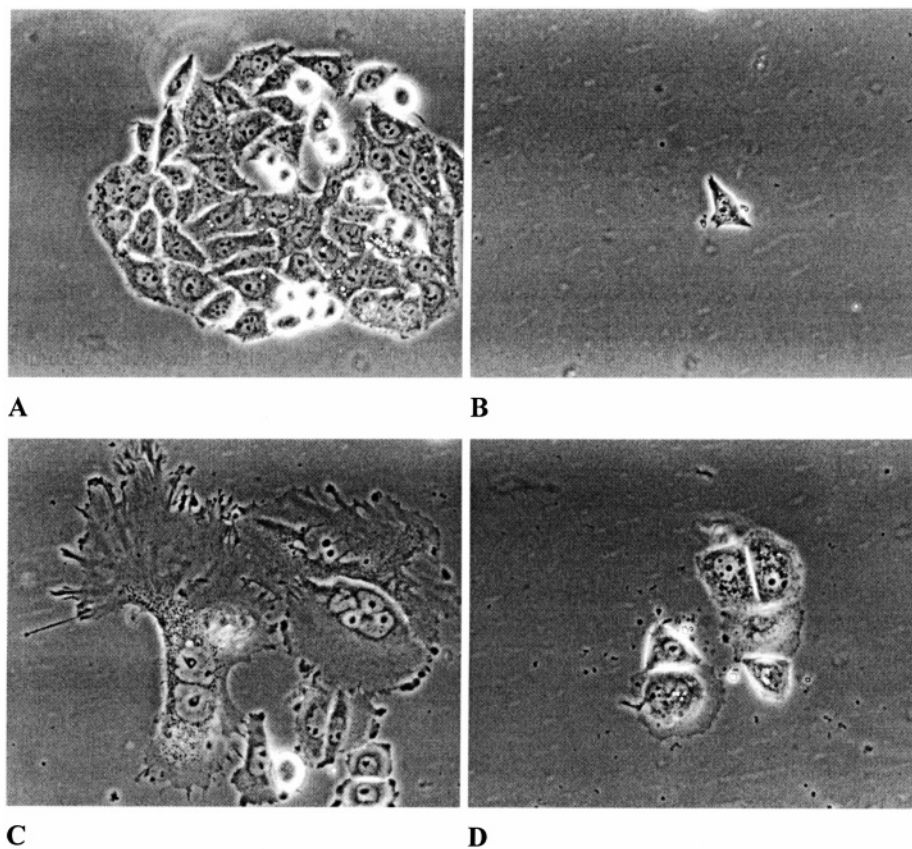


Figure 7. Cell line SISO treated 96 h with various substances: (A) control cells; (B) 1.0 μM 8; (C) 0.5 μM 11; (D) 1.0 μM 7. All pictures are at 400-fold magnification.

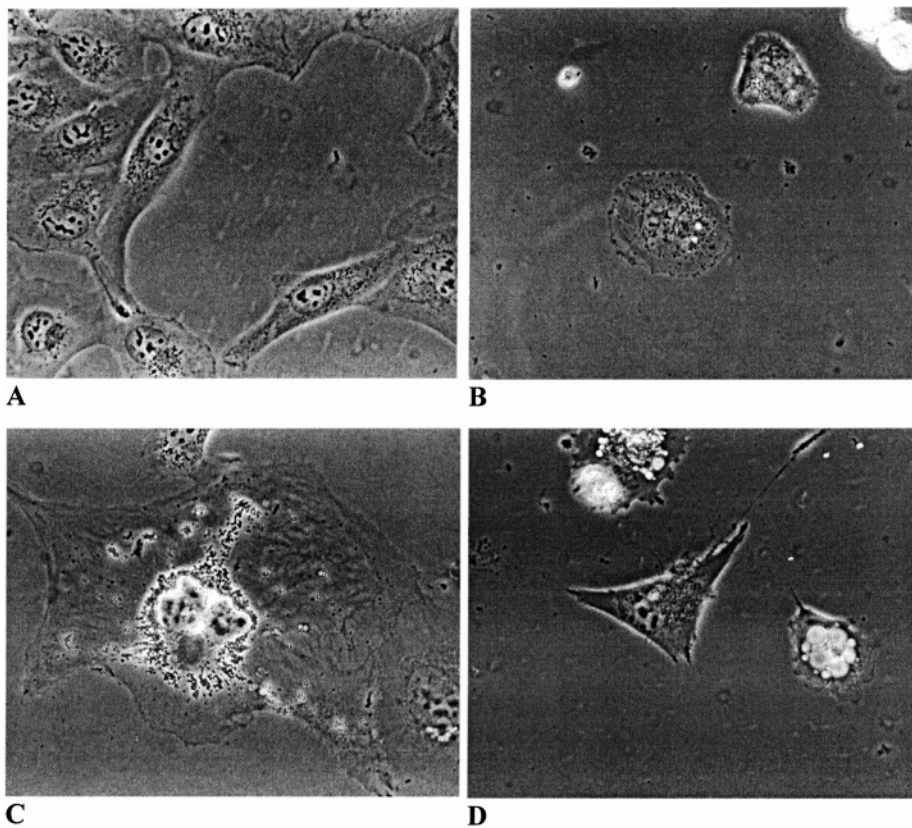


Figure 8. Cell line LCLC-103H treated 96 h with various substances: (A) control cells; (B) 1.0 μM 8; (C) 0.5 μM 11; (D) 1.0 μM 7.

value continued to decrease by 40% between 48 and 72 h (data not shown).

To test further the hypothesis that acrylonitriles are unstable under cell culture conditions, an RP-HPLC

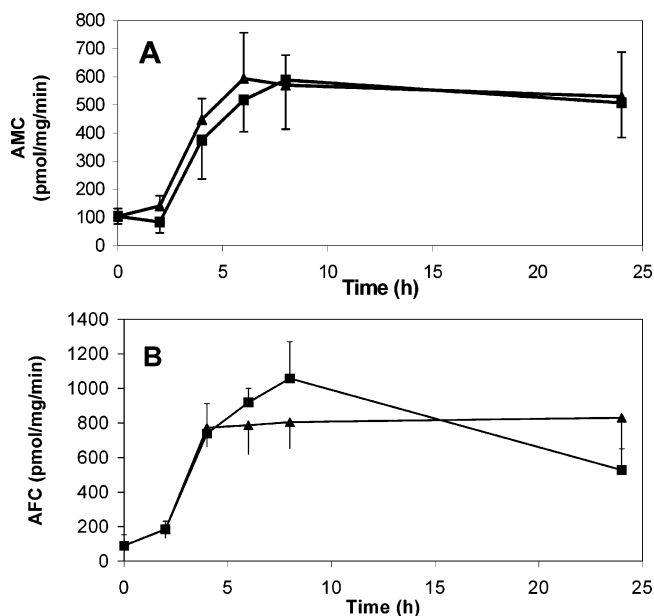


Figure 9. Induction of caspase 3 (A) and caspase 9 (B) activity in HL-60 cells by 8 μ M etoposide (triangles) and 50 μ M compound **11** (squares), respectively. Data points are the averages of three independent experiments. Error bars are ± 1 SD. Activity was measured as the amount of AMC- and AFC-formation that could be inhibited by specific inhibitors for caspases 3 and 9, respectively.

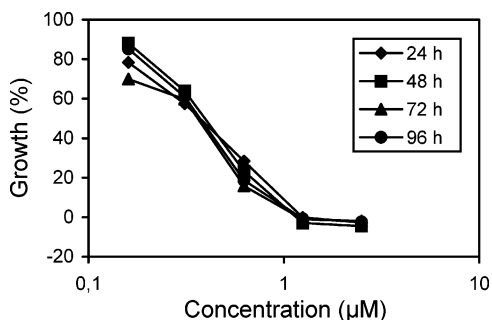


Figure 10. Time-dependent cytotoxicity of **7** in the 5637 cell line.

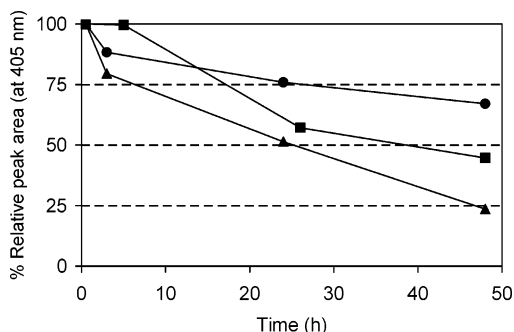


Figure 11. Stability of **10** at 37 $^{\circ}$ C under various cell culture conditions: (●) RPMI medium; (■) medium + 10% FCS; (▲) medium + FCS + 5637 cells. HPLC peak areas were normalized to the peak area at $t = 0$.

assay was developed to monitor compounds **7**, **10**, and **11** in culture medium. Figure 11 shows the results of the HPLC analysis of **10** in RPMI medium, RPMI medium with 10% FCS, or in medium in the presence of 5637 cells. Noticeable time-dependent decreases over the first 24 h were apparent; in particular, when cells were present, the decreases were 50%, 60%, and 90%

for **10**, **7**, and **11**, respectively. There was no evidence for the formation of the respective aldehydes in incubations with RPMI medium (without FCS), indicating that a retro-Knoevenagel reaction is unlikely to occur with these compounds under biological conditions.

Discussion

Some acrylonitriles have previously been reported to possess antitumor properties. Ohsumi and co-workers described various 2,3-diphenylacrylonitriles as combretastatin A-4 analogues that possess tubulin polymerization inhibitory activity and were active on xenografts of the human Grimmdarm tumor in mice.⁸ Another group of acrylonitriles having EGF tyrosine kinase inhibitory activity were described by Gazit and co-workers.¹⁸ This kinase is overexpressed in many malignancies, and thus, such compounds were proposed as antitumor agents. Most recently, Brzozowski and Sączewski described novel acrylonitriles that inhibit the growth of cancer cells.⁹ These acrylonitriles, substituted at position 2 with a triazine ring and at position 3 with a 5-nitrofuranyl ring, served as leads for the present study.

The new acrylonitriles synthesized in this work show interesting in vitro cytotoxic activity on human cancer cells and likely induce cell death by a mechanism of apoptosis. The SAR studies indicate a strong relationship between structure and activity. These studies indicate that the heterocyclic A ring is open for variation such that triazines, triazoles, and benzimidazoles are allowed. In contrast, small changes in the structure of aromatic B ring have large effects on activity. The best aromatic ring system proved to be thiophene, but the type and position of the substituents in the thiophene ring are also critical for activity.

The most active compounds in both groups possess a nitro group in the aromatic B ring, suggesting that this group is somehow involved in the mechanism of action. When Cl or CH₃ are substituted for H at position 5, activity is diminished (compare **16** with **13** and **14**). On the other hand, replacement of H for NO₂ increases dramatically the activity (compare **16** with **11**). This could be due to either differences in electronic or lipophilic properties of these groups; i.e., NO₂ has M-effects while both Cl and CH₃ have M+ effects, but NO₂ is a $-\pi$ group while Cl and CH₃ are both $+\pi$ groups. Interestingly, the position of the nitro group relative to the acrylonitrile in the aromatic ring is critical for activity; substitution at position 2 of the thiophene ring gave the most potent compound (**11**), while substitution at position 3 (**12**) resulted in an isomer almost completely lacking in activity (Table 3). Likewise, the *m*-nitrophenyl derivative **17** was active while the para isomer **18** was devoid of activity (Table 3). These results appear contradictory because active **11** is biosteric with inactive **18** but inactive **12** is biosteric with active **17**.

The highly conjugated system likely forces the A and B rings to lie in a nearly planar orientation to each other. Theoretical calculations with **11** and X-ray crystal structure analysis of **3** and **24** support this idea. However, the barrier to rotation around the bond between the acrylonitrile group and the B ring is relatively low, and interconversion would be expected under biological conditions.

The acrylonitrile functionality is not an absolute requirement for activity, and replacement of the nitrile group for hydrogen (**25**) results in only a ca. 3-fold reduction in potency. However, replacing the nitrile group for a methyl group (compare **11** with **26**) reduces activity dramatically (Tables 3 and 4).

On the basis of the morphological changes in the cells the compounds appear to cause a programmed cell death (apoptosis). Notably, treatment of cells with **11** resulted in a large proportion of giant cells after 96 h (Figures 6C–8C). To confirm the mechanism of cell death, studies on the induction of the activities of caspase 3 and 9 were performed. Both of these enzymes are known to be induced when cancer cells are exposed to antitumor agents, such as etoposide.¹⁶ In this work, we show that at a toxic dose compound **11** causes a time-dependent induction of both caspase activities in the HL-60 leukemia cell line in a manner similar to etoposide (Figure 9).

The selectivity of **11** for cancer cells is not great, as evidenced by the potency in the noncancerous (h-TERT-RPE1 epithelial cell line) cell line compared to the cancer cell lines; the IC₅₀ in the h-TERT cells was only 1.7-fold greater than the average IC₅₀ of all 11 cancer cell lines (0.39 vs 0.23 μ M). However, the selectivities of antitumor agents cisplatin and etoposide for the cancer cell lines were even worse (Table 4); in fact, etoposide was most active on the h-TERT-RPE1 cell line compared to an average of 10 cancer cell lines (0.09 vs 0.54 μ M).

Although the most active compound (**11**) was 10- and 3-fold more potent than cisplatin and etoposide, comparatively the activity is less discriminating over the 11 cancer cell line panel. This is apparent from the relative standard deviations (RSD) of the IC₅₀ values, which are $\pm 91\%$ for cisplatin, $\pm 65\%$ for etoposide, and $\pm 40\%$ for the most active acrylonitrile **11**. The most sensitive cell lines were the 5637 and LCLC-103H, but these cell lines are also quite sensitive to cisplatin. An interesting compound in this respect is **17**, which shows good activity on the LCLC-103H lung cancer cell line (IC₅₀ = 1.13 μ M), i.e., comparable to cisplatin; however, on the remaining cell lines it was only weakly active. It would be interesting to test this compound on additional lung cancer cell lines.

Although it takes several days before morphological changes in the cells become apparent, the compounds achieve their greatest cytotoxic potency within the first 24 h of exposure (Figure 10). This led us to suppose that the compounds were unstable under the culture conditions and unleash their activity during the first 24 h of contact with cells. The time-dependent stabilities of representative compounds (i.e., **7**, **10**, and **11**) were investigated by HPLC methods under various cell culture conditions, i.e., in RPMI medium, in medium with 10% FCS, and in cell culture, respectively. These experiments confirmed that over the first 24 h in cell culture a large fraction of these compounds was lost from the medium (see Figure 11).

Various reactions of acrylonitriles are imaginable, e.g., retro-Knoevenagel reactions, Michael additions with thiols and nitro group reductions. The respective aldehydes were not observed in the HPLC studies, so retro-Knoevenagel reactions appear unlikely. Thiol-

containing substances are known to undergo alkylation reactions with acrylonitrile,^{19,20} and *N*-acetylcysteine is used as an antidote for acrylonitrile poisoning.²¹ Alkylation of sulfur-containing nucleophiles such as glutathione (GSH) and proteins by acrylonitriles, which occur *in vivo*,²² are likely to occur in cell culture as well. Future studies will focus on this possibility. Another metabolic process that could occur is the reduction of the aromatic nitro group by nitro-reductase activities, but this reaction could only be occurring when cells are present.

The initial cellular targets of attack by these compounds are not yet known; however, like other known antitumor agents, **11** caused apoptosis in the HL-60 cell line. Like acrylonitrile, the compounds may act by inhibiting sulfhydryl-dependent enzymes of intermediary metabolism by cyanoethylation of sulfhydryl groups or by liberation of cyanide and subsequent inhibition of cytochrome *c* oxidase.²⁰ However, compounds **25** and **26**, which both lack the nitrile group, are also active. If nonspecific mechanisms were operative, then similar potencies would also be expected over all 12 cell lines. The data presented here, however, appear to favor a selective interaction with a target enzyme or receptor, but more work will be needed to clarify this.

In conclusion, the facile synthesis of acrylonitriles by means of a Koevenagel condensation allowed for the synthesis of a variety of 2,3-disubstituted analogues. A range of cancer cell growth inhibitory activities were observed for the compounds, from potencies 50-fold greater than cisplatin for **11** in the KSYE-510 and the YAPC cell lines down to totally inactive compounds. Importantly, the acrylonitrile functionality is not an absolute requirement for cytotoxic activity as are substituents at position 5 of the triazole ring; thus, this position appears to be free for variations that could lead to compounds with optimal physicochemical and pharmacokinetic properties.

Experimental Section

The acrylonitriles are photosensitive, particularly in organic solutions, and should be stored under protection from light.

Equipment. Melting points were measured on either a Boetius or a MEL-TEMP apparatus and are not corrected. IR spectra were taken in KBr pellets on a Perkin-Elmer FTIR 1600 spectrometer. NMR spectra were recorded on a Varian Gemini 200, a Varian Unity 500, or a Bruker DPX 300 apparatus. ¹H and ¹³C chemical shifts were measured relative to residual solvent signal at 2.50 and 39.5 ppm, respectively. UV-vis spectra were measured in methanol on a Spekol 1200 (Analytik Jena, FRG) apparatus. Unless otherwise noted, analyses of C, H, N were within $\pm 0.4\%$ of the theoretical values.

Cells were automatically counted by using a Coulter Counter Z2 (Beckman-Coulter) instrument. Cell photography was performed with a Axio Vert 25 (Zeiss, FRG) phase-contrast microscope mounted with a Minolta AF camera and fitted with a 40 \times objective.

Preparation of Condensation Products 1–25. Method A. Synthesis of 1,2,4-Triazoles 1–9. Equimolar amounts of (1,2,4-triazol-3-yl)acetonitrile²³ and suitable aldehyde (8.2 mmol) were dissolved in ethanol (15 mL) and treated with piperidine (5 mmol). The reaction mixture was heated under reflux, and then the solvent was evaporated to dryness under reduced pressure. The crude product thus obtained was purified by crystallization from a suitable solvent: DMF (**4**, **5**, **7**), dioxane (**2**), methanol (**6**), ethanol (**1,3**).

According to the above procedure, the following compounds were obtained.

2-(5-Methyl-1*H*-[1,2,4]-triazol-3-yl)-3-(5-nitrofur-2-yl)acrylonitrile (1): from 5-methyl-1*H*-[1,2,4]-triazol-3-yl-acetonitrile (1.0 g, 8.2 mmol) and 5-nitrofurfural (1.15 g, 8.2 mmol); reaction time 2 h; yield 0.31 g (16%); mp 256–260 °C (ethanol); IR, ν 3277 (NH), 3142, 3095, 3054, 2237 (CN), 1522 (NO), 1349 (NO), 1252, 1043 cm^{-1} ; ^1H NMR (DMSO- d_6) δ 2.41 (s, 3H, CH₃), 7.46 (d, 1H, $J = 4.4$ Hz, 3-furyl), 7.83 (d, 1H, $J = 4.4$ Hz, 4-furyl), 8.05 (s, 1H, =CH), 14.16 (s, 1H, NH); UV-vis, λ_{max} 245, 364 nm ($\log \epsilon = 4.36$); HPLC, $t_{\text{R}} = 7.12$ min. Anal. (C₁₀H₇N₅O₃ (245.19)) C, H, N. N: calcd 28.57; found 29.62.

2-(5-Methyl-1*H*-[1,2,4]-triazol-3-yl)-3-(5-nitrothiophen-2-yl)acrylonitrile (2): from 5-methyl-1*H*-[1,2,4]-triazol-3-yl-acetonitrile (1.0 g, 8.2 mmol) and 5-nitro-2-thiophene-carboxaldehyde (1.15 g, 8.2 mmol); reaction time 2 h; yield 0.54 g (26%); mp 278–280 °C (dioxane); IR, ν 3307 (NH), 3095, 3072, 3030, 2225 (CN), 1504 (NO), 1328 (NO), 1246, 1078 cm^{-1} ; ^1H NMR (DMSO- d_6) δ 2.41 (s, 3H, CH₃), 7.89 (d, 1H, $J = 4.4$ Hz, 3-thienyl), 8.21 (d, 1H, $J = 4.4$ Hz, 4-thienyl), 8.46 (s, 1H, =CH), 14.15 (s, 1H, NH); UV-vis, λ_{max} 273, 379 nm ($\log \epsilon = 4.38$); HPLC, $t_{\text{R}} = 9.79$ min. Anal. (C₁₀H₇N₅O₂S₁ (261.27)) C, H, N.

2-(5-Methyl-1*H*-[1,2,4]-triazol-3-yl)-3-(3-nitrophenyl)acrylonitrile (3): from 5-methyl-1*H*-[1,2,4]-triazol-3-yl-acetonitrile (1.0 g, 8.2 mmol) and 3-nitrobenzaldehyde (1.24 g, 8.2 mmol); reaction time 3 h; yield 0.57 g (28%); mp 181–182 °C (ethanol); IR, ν 3154 (NH), 3077, 3025, 3030, 2220 (CN), 1525 (NO), 1347 (NO), 1163, 1061 cm^{-1} ; ^1H NMR (DMSO- d_6) δ 2.42 (s, 3H, CH₃), 7.81–7.85 (m, 1H, Ar-H), 8.32–8.36 (m, 3H, Ar-H), 8.86 (s, 1H, =CH), 14.09 (s, 1H, NH); UV-vis, λ_{max} 299 nm ($\log \epsilon = 4.34$); HPLC, $t_{\text{R}} = 8.79$ min. Anal. (C₁₂H₉N₅O₂ (255.24)) C, H, N.

2-(5-Phenyl-1*H*-[1,2,4]-triazol-3-yl)-3-(5-nitrofur-2-yl)acrylonitrile (4): from 5-phenyl-1*H*-[1,2,4]-triazol-3-yl-acetonitrile (1.0 g, 5.4 mmol) and 5-nitrofurfural (0.77 g, 5.4 mmol); reaction time 1 h; yield 0.32 g (19%); mp 284–286 °C (DMF); IR, ν 3213 (NH), 3154, 3048, 2225 (CN), 1522 (NO), 1349 (NO), 1258, 1122, 1031 cm^{-1} ; ^1H NMR (DMSO- d_6) δ 7.53 (d, 1H, $J = 4.0$ Hz, 3-furyl), 7.56–7.62 (m, 3H, Ar-H), 7.87 (d, 1H, $J = 4.0$ Hz, 4-furyl), 8.01–8.08 (m, 2H, Ar-H), 8.19 (s, 1H, =CH), 15.00 (s, 1H, NH); UV-vis, λ_{max} 239, 372 nm ($\log \epsilon = 4.39$); HPLC, $t_{\text{R}} = 14.72$ min. Anal. (C₁₅H₉N₅O₃ (307.26)) C, H, N.

2-(5-Phenyl-1*H*-[1,2,4]-triazol-3-yl)-3-(5-nitrothiophen-2-yl)acrylonitrile (5): from 5-phenyl-1*H*-[1,2,4]-triazol-3-yl-acetonitrile (1.0 g, 5.4 mmol) and 5-nitro-2-thiophenecarboxaldehyde (0.85 g, 5.4 mmol); reaction time 0.5 h; yield 1.08 g (62%); mp 295–296 °C (DMF); IR, ν 3230 (NH), 3101, 2931, 2220 (CN), 1651, 1501 (NO), 1337 (NO), 1208, 1116, 1031 cm^{-1} ; ^1H NMR (DMSO- d_6) δ 7.56–7.62 (m, 3H, Ar-H), 7.96 (d, 1H, $J = 4.6$ Hz, 3-thienyl), 8.03–8.08 (m, 2H, Ar-H), 8.25 (d, 1H, $J = 4.6$ Hz, 4-thienyl), 8.58 (s, 1H, =CH), 15.00 (s, 1H, NH); UV-vis, λ_{max} 240, 386 nm ($\log \epsilon = 4.34$); HPLC, $t_{\text{R}} = 23.36$ min. Anal. (C₁₅H₉N₅O₂S (323.34)) C, H, N.

2-(5-Phenyl-1*H*-[1,2,4]-triazol-3-yl)-3-(3-nitrophenyl)acrylonitrile (6): from 5-phenyl-1*H*-[1,2,4]-triazol-3-yl-acetonitrile (1.0 g, 5.4 mmol) and 3-nitrobenzaldehyde (0.82 g, 5.4 mmol); reaction time 2 h; yield 0.80 g (47%); mp 279–281 °C (methanol); IR, ν 3136 (NH), 3089, 3007, 2936, 2220 (CN), 1525 (NO), 1354 (NO), 1137, 996, 943 cm^{-1} ; ^1H NMR (DMSO- d_6) δ 7.56–7.63 (m, 3H, Ar-H), 7.84 (t, 1H, Ar-H), 8.04–8.08 (m, 2H, Ar-H), 8.33–8.46 (m, 3H, Ar-H), 8.89 (s, 1H, =CH), 14.91 (s, 1H, NH); UV-vis, λ_{max} 258, 308 nm ($\log \epsilon = 4.44$); HPLC, $t_{\text{R}} = 21.46$ min. Anal. (C₁₇H₁₁N₅O₂ (317.31)) C, H, N.

2-(5-Benzyl-1*H*-[1,2,4]-triazol-3-yl)-3-(5-nitrothiophen-2-yl)acrylonitrile (7): from 5-benzyl-1*H*-[1,2,4]-triazol-3-yl-acetonitrile (1.0 g, 5.0 mmol) and 5-nitro-2-thiophenecarboxaldehyde (0.79 g, 5.0 mmol); reaction time 2 h; yield 0.35 g (21%); mp 219–220 °C (DMF); IR, ν 3250 (NH), 3107, 3036, 2966, 2848, 2214 (CN), 1501 (NO), 1334 (NO), 1211, 1114, 1034, 867 cm^{-1} ; ^1H NMR (DMSO- d_6) δ 4.15 (s, 2H, CH₂), 7.22–7.38 (m, 5H, Ar-H), 7.91 (d, 1H, $J = 4.3$ Hz, 3-thienyl), 8.21 (d, 1H, $J = 4.3$ Hz, 4-thienyl), 8.45 (s, 1H, =CH), 14.40 (s, 1H, NH); UV-vis, λ_{max} 273, 380 nm ($\log \epsilon = 4.24$); HPLC, $t_{\text{R}} = 15.73$ min. Anal. (C₁₆H₁₁N₅O₂S (337.37)) C, H, N.

2-(5-Benzyl-1*H*-[1,2,4]-triazol-3-yl)-3-(5-nitrofur-2-yl)acrylonitrile (8): from 5-benzyl-1*H*-[1,2,4]-triazol-3-yl-

acetonitrile (1.0 g, 5 mmol) and 5-nitrofurfural (0.7 g, 5 mmol); reaction time 2 h; yield 0.65 g (58%); mp 188–190 °C (methanol) (ref 3 mp 188–190 °C); IR, ν 3242 (NH), 3130, 3048, 2919, 2231 (CN), 1537 (NO), 1346 (NO), 1246, 1014, 811, 705 cm^{-1} ; ^1H NMR δ 4.15 (s, 1H, CH₂), 7.20–7.40 (m, 5H, Ar-H), 7.48 (d, $J = 3.8$ Hz, 1H, 3-furyl), 7.83 (d, $J = 3.8$ Hz, 1H, 4-furyl), 8.06 (s, 1H, =CH), 14.40 (s, 1H, NH); UV-vis, λ_{max} 245, 366 nm ($\log \epsilon = 4.30$); HPLC, $t_{\text{R}} = 11.33$ min. Anal. (C₁₆H₁₁N₅O₂S (321.29)) C, H, N.

2-(5-Benzyl-1*H*-[1,2,4]-triazol-3-yl)-3-(4-dimethylaminophenyl)acrylonitrile (9): from 5-benzyl-1*H*-[1,2,4]-triazol-3-yl-acetonitrile (1.0 g, 5 mmol) and 4-dimethylaminobenzaldehyde (0.75 g, 5 mmol); reaction time 2 h; yield 1.0 g (65%); mp 199–200 °C (dioxane) (ref 3 mp 199–200 °C); IR, ν 3451, 3061, 2907, 2213 (CN), 1584, 1528 (NO), 1327 (NO), 1193, 816, 724 cm^{-1} ; ^1H NMR (DMSO- d_6): δ 3.0 (s, 6H, N(CH₃)₂), 4.1 (s, 2H, CH₂), 6.80 (d, 2H, $J = 8.9$ Hz, Ar-H), 7.20–7.40 (m, 5H, Ar-H), 7.8 (d, 2H, $J = 8.9$ Hz, Ar-H), 7.96 (s, 1H, =CH), 14.00 (s, 1H, NH); UV-vis, λ_{max} 256, 391 nm ($\log \epsilon = 4.47$); HPLC, $t_{\text{R}} = 12.61$ min. Anal. (C₁₆H₁₁N₅O₂S (329.44)) C, H, N.

Method B. Synthesis of Benzimidazoles 10–23. To an equimolar amount of (benzimidazol-2-yl)acetonitrile²⁴ and corresponding aldehyde (6.4 mmol) dissolved in ethanol (20 mL) was added 10% methanolic KOH (10 mmol), and the reaction mixture was kept at room temperature for 0.5 h. In the cases of **13** and **14**, heating under reflux was required. Then the solution was cooled to 5 °C and the product that precipitated was collected by filtration and purified by recrystallization from a suitable solvent: ethanol (**15**, **16**, **20–23**), ethanol/DMF (**12**, **17**, **19**), DMF (**10**, **11**), acetone (**18**).

According to the above procedure, the following compounds were obtained.

2-(1*H*-Benzimidazol-2-yl)-3-(5-nitrofur-2-yl)acrylonitrile (10): from (benzimidazol-2-yl)acetonitrile (1.0 g, 6.4 mmol) and 5-nitrofurfural (0.90 g, 6.4 mmol); yield 0.84 g (47%); mp 319–322 °C dec (ref 5a mp 312–313 °C dec); IR, ν 3265 (NH), 3154, 3048, 2243 (CN), 1522 (NO), 1469, 1349 (NO), 1263, 1178, 1031, 808, 735 cm^{-1} ; UV-vis, λ_{max} 317, 405 nm ($\log \epsilon = 4.44$); HPLC, $t_{\text{R}} = 10.51$ min. Anal. (C₁₄H₈N₄O₃ (280.23)) C, H, N.

2-(1*H*-Benzimidazol-2-yl)-3-(5-nitrothiophen-2-yl)acrylonitrile (11): from (benzimidazol-2-yl)acetonitrile (1.1 g, 7.0 mmol) and 5-nitro-2-thiophenecarboxaldehyde (1.1 g, 7.0 mmol); yield 1.47 g (71%); mp 348–350 °C dec; IR, ν 3277 (NH), 3107, 3048, 2231 (CN), 1513 (NO), 1334 (NO), 1225, 1119, 1028, 817, 729, 623 cm^{-1} ; ^1H NMR (DMSO- d_6) δ 7.25–7.33 (m, 2H, Ar-H), 7.62–7.67 (m, 3H, Ar-H), 7.84 (d, 1H, $J = 4.5$ Hz, 3-thienyl), 8.25 (d, 1H, $J = 4.5$ Hz, 4-thienyl), 8.59 (s, 1H, =CH), 13.25 (s, 1H, NH); UV-vis, λ_{max} 300, 417 nm ($\log \epsilon = 4.28$); HPLC, $t_{\text{R}} = 13.68$ min. Anal. (C₁₄H₈N₄O₂S (296.31)) C, H, N.

2-(1*H*-Benzimidazol-2-yl)-3-(2-nitrothiophen-4-yl)acrylonitrile (12): from 0.595 g (3.8 mmol) of (benzimidazol-2-yl)acetonitrile and 5-nitro-3-thiophenecarboxaldehyde (0.595 g, 3.8 mmol) without added KOH; yield 0.66 g (59%); yellow crystals; mp 236–239 °C dec; IR, ν 3296 (NH), 3112, 2231 (CN), 1536 (NO), 1500, 1346 (NO), 1218, 1088, 769, 584 cm^{-1} ; ^1H NMR (DMSO- d_6) δ 7.24–7.28 (m, 2H, Ar-H); 7.58–7.64 (m, 2H, Ar-H); 8.32 (s, 1H, =CH), 8.64 (s, 1H, thienyl), 8.65 (s, 1H, thienyl), 13.12 (bs, 1H, NH); UV-vis, λ_{max} = 271, 349 nm ($\log \epsilon = 3.74$); HPLC, $t_{\text{R}} = 13.17$ min ($\lambda = 349$ nm). Anal. (C₁₄H₈N₄O₂S (296.31)) C, H, N, S. C: calcd 56.74; found 56.22. S: calcd 10.82; found 11.02.

2-(1*H*-Benzimidazol-2-yl)-3-(5-chlorothiophen-2-yl)acrylonitrile (13): from 0.20 g (1.27 mmol) of (1*H*-benzimidazol-2-yl)acetonitrile and 0.187 g 5-chloro-2-thiophenecarboxaldehyde (1.27 mmol); yield 0.20 g (55%); green needles from ethanol; mp 283–284 °C dec; IR, ν 3267 (NH), 3047, 2230 (CN), 1586, 1434, 1410, 1320, 1228, 1005, 906, 743; ^1H NMR (DMSO- d_6) δ 7.26–7.10 (m, 2H, Ar-H), 7.41 (d, 1H, $J = 4.2$ Hz, thienyl), 7.59–7.61 (m, 2H, Ar-H), 7.72 (d, 1H, $J = 4.2$ Hz, thienyl), 8.48 (s, 1H, =CH), 13.05 (bs, 1H, NH); UV-vis, λ_{max} 277, 381 nm ($\log \epsilon = 4.38$) HPLC, $t_{\text{R}} = 23.44$ min. Anal. (C₁₄H₈ClN₃S (285.76)) C, H, N. H: calcd 2.83; found 3.37.

2-(1H-Benzimidazol-2-yl)-3-(5-methylthiophen-2-yl)acrylonitrile (14): from 0.20 g (1.27 mmol) of (1H-benzimidazol-2-yl)acetonitrile and 0.16 g of 5-methyl-2-thiophenecarboxaldehyde (1.27 mmol); yield 0.161 g (48%); yellow needles from ethanol; mp 273–275 °C; IR, ν 3277 (NH), 3048, 2917, 2229 (CN), 1590, 1439, 1322, 1276, 1230, 1160, 1050, 748; ^1H NMR (DMSO- d_6) δ 2.60 (s, 3H, CH₃), 7.06 (d, 1H, J = 4.2 Hz, thienyl), 7.34–7.38 (m, 2H, Ar–H), 7.57–7.59 (m, 2H, Ar–H), 7.61 (d, 1H, J = 4.2 Hz, thienyl), 8.45 (s, 1H, =CH), 12.97 (bs, 1H, NH); UV-vis, λ_{max} 281, 381 nm (log ϵ = 4.39) HPLC, t_{R} = 16.24. Anal. (C₁₅H₁₁N₃S (265.35)) C, H, N, H: calcd 4.19; found 4.97.

2-(1H-Benzimidazol-2-yl)-3-(furan-2-yl)acrylonitrile (15): from (benzimidazol-2-yl)acetonitrile (0.5 g, 3.2 mmol) and furfural (0.31 g, 3.2 mmol); yield 0.38 g (51%); mp 192–194 °C (ref 5a mp 194–195.5 °C); IR, ν 3500–3300, 2225 (CN), 1625, 1611, 1442, 1279, 1021, 746 cm⁻¹; ^1H NMR (DMSO- d_6) δ 6.85 (dd, 1H, 4-furyl), 7.19–7.31 (m, 2H, Ar–H), 7.36 (d, 1H, 5-furyl), 7.49–7.60 (m, 1H, Ar–H), 7.61–7.72 (m, 1H, Ar–H), 8.13 (d, 1H, 3-furyl), 8.16 (s, 1H, =CH), 13.01 (bs, 1H, NH); UV-vis, λ_{max} 278, 374 nm (log ϵ 4.47); HPLC, t_{R} = 10.07 min. Anal. (C₁₄H₉N₃O (234.24)) C, H, N, C: calcd 71.47; found 66.49. N: calcd 17.87; found 16.68.

2-(1H-Benzimidazol-2-yl)-3-(thiophen-2-yl)acrylonitrile (16): from (benzimidazol-2-yl)acetonitrile (0.28 g, 1.8 mmol) and 2-thiophenecarboxaldehyde (0.20 g, 1.8 mmol); yield 0.20 g (45%); mp 222–224 °C (ref 25 mp 216–218 °C); IR, ν 3500–3200, 2218 (CN), 1624, 1594, 1442, 1411, 1327, 1051, 746 cm⁻¹; ^1H NMR (DMSO- d_6) δ 7.20–7.29 (m, 2H, Ar–H), 7.34 (dd, 1H, 4-thienyl), 7.50–7.73 (m, 2H, Ar–H), 7.85 (d, 1H, 5-thienyl), 8.07 (d, 1H, 3-thienyl), 8.56 (s, 1H, =CH), 13.02 (bs, 1H, NH); UV-vis, λ_{max} 282, 370 nm (log ϵ 4.39); HPLC, t_{R} = 12.19. Anal. (C₁₄H₉N₃S (251.33)) C, H, N, C: calcd 66.90; found 62.74. N: calcd 16.72; found 15.72.

2-(1H-Benzimidazol-2-yl)-3-(3-nitrophenyl)acrylonitrile (17): from (benzimidazol-2-yl)acetonitrile (0.28 g, 1.8 mmol) and 3-nitrobenzaldehyde (0.27 g, 1.8 mmol); yield 0.38 g (74%); mp 256–258 °C (ref 5a mp 263–265 °C); IR, ν 3500–3200, 2232 (CN), 1625, 1528 (NO), 1439, 1349 (NO), 1104, 752, 669 cm⁻¹; ^1H NMR (DMSO- d_6) δ 7.28–7.31 (m, 2H, Ar–H), 7.59–7.72 (m, 2H, Ar–H), 7.88–7.95 (t, 1H, Ar–H), 8.35–8.42 (m, 2H, Ar–H), 8.50 (s, 1H, =CH), 8.84–8.85 (m, 1H, Ar–H), 13.19 (bs, 1H, NH); UV-vis, λ_{max} 260, 351 nm (log ϵ 4.35); HPLC, t_{R} = 13.37 min. Anal. (C₁₆H₁₀N₄O₂ (290.28)) C, H, N.

2-(1H-Benzimidazol-2-yl)-3-(4-nitrophenyl)acrylonitrile (18): from (benzimidazol-2-yl)acetonitrile (0.28 g, 1.8 mmol) and 4-nitrobenzaldehyde (0.27 g, 1.8 mmol); yield 0.42 g (81%); mp >300 °C (ref 5a mp 320–321 °C); IR, ν 3444, 3262 (NH), 2243 (CN), 1651, 1516 (NO), 1440, 1346 (NO), 1117, 908, 836, 771, 635 cm⁻¹; ^1H NMR (DMSO- d_6) δ 7.26–7.37 (m, 2H, Ar–H), 7.56–7.77 (m, 2H, Ar–H), 8.20 (d, 2H, J = 9.2 Hz, Ar–H), 8.43 (d, 2H, J = 9.2 Hz, Ar–H), 8.47 (s, 1H, =CH), 13.20 (bs, 1H, NH); UV-vis, λ_{max} 280, 371 nm (log ϵ 4.25); HPLC, t_{R} = 13.6 min. Anal. (C₁₆H₁₀N₄O₂ (290.28)) C, H, N.

2-(1H-Benzimidazol-2-yl)-3-(4-dimethylaminophenyl)acrylonitrile (19): from (benzimidazol-2-yl)acetonitrile (0.30 g, 1.9 mmol) and 4-dimethylaminobenzaldehyde (0.28 g, 1.9 mmol); yield 0.27 g (49%); mp >300 °C (ref 5a mp 313–314 °C); IR, ν 3445, 3249 (NH), 2225 (CN), 1614, 1589, 1537, 1450, 1379, 1276, 1203, 810, 727 cm⁻¹; ^1H NMR (DMSO- d_6) δ 2.96 (s, 6H, N(CH₃)₂), 6.86 (d, 2H, J = 9.1 Hz, Ar–H), 7.17–7.23 (m, 2H, Ar–H), 7.48–7.63 (m, 2H, Ar–H), 7.90 (d, 2H, J = 9.1 Hz, Ar–H), 8.13 (s, 1H, =CH), 12.79 (bs, 1H, NH); UV-vis, λ_{max} 430 nm (log ϵ 4.53); HPLC, t_{R} = 20.71 min. Anal. (C₁₈H₁₆N₄ (288.38)) C, H, N.

2-(1H-Benzimidazol-2-yl)-3-(4-cyanophenyl)acrylonitrile (20): from (benzimidazol-2-yl)acetonitrile (0.30 g, 1.9 mmol) and 4-cyanobenzaldehyde (0.25 g, 1.9 mmol); yield 0.29 g (56%); mp 270–272 °C; IR, ν 3442, 3330, (NH), 3077, 2234 (CN), 1626, 1415, 1319, 913, 740, 546 cm⁻¹; ^1H NMR (DMSO- d_6) δ 7.25–7.34 (m, 2H, Ar–H), 7.55–7.77 (m, 2H, Ar–H), 8.05 (d, 2H, J = 8.6 Hz, Ar–H), 8.13 (d, 2H, J = 8.6 Hz, Ar–H), 8.42 (s, 1H, =CH), 13.24 (bs, 1H, NH); UV-vis, λ_{max} 276, 358

nm (log ϵ = 4.43); HPLC, t_{R} = 10.58 min. Anal. (C₁₇H₁₀N₄ (270.31)) C, H, N.

2-(1H-Benzimidazol-2-yl)-3-(4-methoxyphenyl)acrylonitrile (21): from (benzimidazol-2-yl)acetonitrile (0.25 g, 1.6 mmol) and 4-methoxybenzaldehyde (0.22 g, 1.6 mmol); yield 0.27 g (61%); mp 227–229 °C (ref 26 mp 235 °C); IR, ν 3444, 3182 (NH), 2840, 2220 (CN), 1591, 1509, 1442, 1263, 1179, 1031, 829, 744 cm⁻¹; ^1H NMR (DMSO- d_6) δ 3.88 (s, 3H, CH₃), 7.16 (d, 2H, J = 9.8 Hz, Ar–H), 7.22–7.31 (m, 2H, Ar–H), 7.51–7.75 (m, 2H, Ar–H), 8.01 (d, 2H, J = 9.8 Hz, Ar–H), 8.28 (s, 1H, =CH), 13.01 (s, 1H, NH); UV-vis, λ_{max} 263, 366 nm (log ϵ 4.34); HPLC, t_{R} = 15.07 min. Anal. (C₁₇H₁₃N₃O (275.32)) C, H, N, C: calcd 74.16; found 69.88. N: calcd 15.27; found 14.46.

2-(1H-Benzimidazol-2-yl)-3-(4-trifluoromethoxyphenyl)acrylonitrile (22): from (benzimidazol-2-yl)acetonitrile (0.30 g, 1.9 mmol) and 4-trifluoromethoxybenzaldehyde (0.36 g, 1.9 mmol); yield 0.27 g (44%); mp 247–248 °C; IR, ν 3444, 3268 (NH), 2239 (CN), 1609, 1506, 1438, 1282, 1206, 1165, 908, 748, 630 cm⁻¹; ^1H NMR (DMSO- d_6) δ 7.26–7.31 (m, 2H, Ar–H), 7.60–7.70 (d, 2H, J = 8.4 Hz, Ar–H, m, 2H, Ar–H), 8.12 (d, 2H, J = 8.4 Hz, Ar–H), 8.39 (s, 1H, =CH), 13.13 (bs, 1H, NH); UV-vis, λ_{max} 274, 348 nm (log ϵ 4.22); HPLC, t_{R} = 25.95 min. Anal. (C₁₇H₁₀F₃N₃O (329.29)) C, H, N.

2-(1H-Benzimidazol-2-yl)-3-(4-trifluoromethylphenyl)acrylonitrile (23): from (benzimidazol-2-yl)acetonitrile (0.30 g, 1.9 mmol) and 4-trifluoromethylbenzaldehyde (0.33 g, 1.9 mmol); yield 0.31 g (52%); mp 258–260 °C; IR, ν 3444, 3277 (NH), 2241 (CN), 1626, 1438, 1331, 1162, 1117, 1071, 911, 830, 748 cm⁻¹; ^1H NMR (DMSO- d_6) δ 7.27–7.32 (m, 2H, Ar–H), 7.59–7.71 (m, 2H, Ar–H), 7.98 (d, 2H, J = 8.3 Hz, Ar–H), 8.16 (d, 2H, J = 8.3 Hz, Ar–H), 8.44 (s, 1H, =CH), 13.16 (bs, 1H, NH); UV-vis, λ_{max} 269, 350 nm (log ϵ 4.40); HPLC, t_{R} = 22.38 min. Anal. (C₁₇H₁₀F₃N₃ (313.30)) C, H, N.

Method C. Synthesis of Benzimidazoles 24 and 26. A solution of 5-nitrothiophene-2-carboxaldehyde (3.8 mmol) and an equimolar amount of corresponding 2-alkylbenzimidazole in acetic anhydride (15 mL) was heated under reflux for 3 h. The solution was evaporated to dryness under reduced pressure, and the resulting oily residue was purified by crystallization from ethanol in the presence of charcoal.

According to the above procedure, the following compounds were obtained.

1-Acetyl-2-[2-(5-nitrothiophen-2-yl)vinyl]-1H-benzimidazole (24): from 2-methylbenzimidazole (0.5 g, 3.8 mmol) and 5-nitro-2-thiophenecarboxaldehyde (0.6 g, 3.8 mmol); yield 0.5 g (42%); mp 171–173 °C; IR, ν 3085, 1721, 1488, 1331 (NO), 1290, 1033, 963, 806, 750 cm⁻¹; ^1H NMR (CDCl₃) δ 2.90 (s, 3H, CH₃), 7.20 (d, J = 3.9, 1H, 3-thienyl), 7.40–7.46 (m, 2H, Ar–H), 7.68–7.73 (m, 1H, Ar–H), 7.78–7.82 (m, 1H, Ar–H), 7.85–7.90 (d, d, =CH, 4-thienyl), 7.97 (d, J = 15.5 Hz, =CH). Anal. (C₁₅H₁₁N₃O₃S (313.2)) C, H, N.

2-[1-Methyl-2-(5-nitrothiophen-2-yl)vinyl]-1H-benzimidazole (26): from 2-ethylbenzimidazole (0.5 g, 3.4 mmol) and 5-nitro-2-thiophenecarboxaldehyde (0.54 g, 3.4 mmol); yield 0.8 g (80%); mp 235–237 °C; IR, ν 3472 (NH), 1723, 1487, 1424, 1340 (NO), 1189, 1034, 731 cm⁻¹; ^1H NMR (DMSO- d_6) δ 2.57 (s, 3H, CH₃), 7.21–7.24 (m, 2H, Ar–H), 7.44 (d, 1H, J = 4.4 Hz, 3-thienyl), 7.51–7.74 (m, 2H, Ar–H), 7.87 (s, 1H, =CH), 8.20 (d, 1H, J = 4.4 Hz, 4-thienyl), 12.81 (bs, 1H, NH); UV-vis, λ_{max} 295, 407 nm (log ϵ 4.45); HPLC, t_{R} = 16.87 min. Anal. (C₁₄H₁₁N₃O₂S (285.33)) C, H, N, C: calcd 58.93; found 55.55. H: calcd 3.89; found 4.52. N: calcd 14.73; found 13.98.

Method D. 2-[2-(5-Nitrothiophen-2-yl)vinyl]-1H-benzimidazole (25) was obtained according to the procedure described by Porousek.¹⁰ 2-[(Triphenylphosphonium chloride)-methyl]benzimidazole was subjected to a reaction with 5-nitro-2-thiophenecarboxaldehyde in the presence of sodium methoxide in methanol at room temperature to give **23**, which melted at 228–230 °C (ref 10 mp 193–194 °C); IR, ν 3105, 1631, 1522, 1501, 1430, 1349, 1323, 1202, 1039, 955 cm⁻¹; ^1H NMR (DMSO- d_6) δ 7.18–7.26 (m, 2H, Ar–H), 7.32 (d, J = 16.2 Hz, 1H, =CH), 7.50–7.64 (m, 2H, Ar–H), 7.54 (d, J = 4.0 Hz, 1H, 3-thienyl), 7.83 (d, J = 16.2 Hz, 1H, =CH), 8.14 (d, J =

4.0 Hz, 1H, 4-thienyl), 12.8 (s, 1H, NH). Anal. (C₁₃H₉N₃O₂S (271.3)) C, H, N.

X-ray Crystallography of 3 and 24. Crystal Data for C₁₂H₉N₃O₂ (3). Orthorhombic, space group *Pbca*, $a = 9.2700(4)$ Å, $b = 13.7023(6)$ Å, $c = 18.3866(7)$ Å, $V = 2335.5(2)$ Å³, $Z = 8$, $d_x = 1.452$ g·cm⁻³, $T = 110$ K. Data were collected for a crystal with dimensions 0.25 mm × 0.25 mm × 0.05 mm on a KumaCCD diffractometer using graphite monochromated Mo Kα radiation. Final *R* indices for 2112 reflections with $I > 2\sigma(I)$ and 209 refined parameters are the following: $R1 = 0.0480$, $wR2 = 0.10085$ ($R1 = 0.0591$, $wR2 = 0.1067$ for all 2382 data).

Crystal Data for C₁₅H₁₁N₃O₃S (24). Triclinic, space group *P1̄*, $a = 6.5988(6)$ Å, $b = 8.3769(7)$ Å, $c = 13.0684(11)$ Å, $\alpha = 94.580(7)^\circ$, $\beta = 99.949(7)^\circ$, $\gamma = 102.076(7)^\circ$, $V = 690.72(10)$ Å³, $Z = 2$, $d_x = 1.507$ g·cm⁻³, $T = 130$ K. Data were collected for a crystal with dimensions 0.35 mm × 0.25 mm × 0.01 mm on a KumaCCD diffractometer using graphite monochromated Mo Kα radiation. Final *R* indices for 2237 reflections with $I > 2\sigma(I)$ and 243 refined parameters are the following: $R1 = 0.0407$, $wR2 = 0.0870$ ($R1 = 0.0588$, $wR2 = 0.0952$ for all 2809 data).

Cytotoxicity Studies. All cell culture reagents were purchased from Sigma (Deisenhofen, FRG). Cancer cell lines were obtained from the German Collection of Microorganisms and Cell Cultures (DSMZ) (Braunschweig, FRG). The h-TERT-RPE1 cell line was obtained from Clontech (Heidelberg, FRG). The culture medium was RPMI-1640 medium except for the h-TERT-RPE1 cell line, where DMEM/F-12 medium was used. All mediums were supplemented with 2 g/L NaHCO₃ and 10% FCS. For the MCF-7 cell line, the RPMI medium was supplemented with 1 mM pyruvate, MEM salts, and amino acids. Cells were grown in 75 cm² plastic culture flasks (Sarstedt, Nümbrecht, FRG) in a humid atmosphere of 5% CO₂ at 37 °C and passaged shortly before becoming confluent. Cytotoxicity determinations are based on cellular staining with crystal violet and were performed as previously described.¹⁷ Briefly, a volume of 100 μL of a cell suspension was seeded into 96-well microtiter plates (Sarstedt) at a density of 1000 cells per well except for the LCLC-103H and KYSE-510 cell lines, which were plated out at 250 and 500 cells per well, respectively. Twenty-four hours later, cells were exposed to the substance at five dilutions (geometric) continuously for the next 96 h. At the end of the exposure time, the medium was removed and the cells were fixed with a glutaraldehyde solution. The cells were then stained with crystal violet and the OD was measured at $\lambda = 570$ nm with a 2010 plate reader (Anthos).

The percent growth values were calculated by the equation

$$\text{growth (\%)} = \frac{\text{OD}_T - \text{OD}_{c,0}}{\text{OD}_c - \text{OD}_{c,0}} \times 100$$

where OD_T is the mean absorbance of the treated cells, OD_c is the mean absorbance of the controls, and OD_{c,0} is the mean absorbance at the time the drug was added. The IC₅₀ values were estimated by a linear least-squares regression of the growth values versus the logarithm of the substance concentration; only concentrations that yielded growth values between 10% and 90% were used in the calculation. The reported IC₅₀ values are the average of two to three independent experiments, and these varied less than 20% from the individual values.

Caspase Induction Studies. HL-60 human acute myeloid leukemia cells (DSMZ) were maintained in logarithmic growth in RPMI 1640 supplemented with 10% fetal bovine serum, 30 mg/L of penicillin G, and 40 mg/L of streptomycin sulfate. Apoptosis was induced by treatment (1 × 10⁵ cells/mL) with 8 μM etoposide or 50 μM compound 11. IC₅₀ values determined with an MTT assay for etoposide and compound were 1 and 20 μM, respectively. Cells were incubated in a humid atmosphere of 5% CO₂ at 37 °C, and the cell lysates were prepared at 0, 2, 4, 6, 8, and 24 h after treatment.

For the preparation of the cell-free extracts, all steps were performed at 4 °C. Cells were pelleted at 500g for 4 min, washed with PBS, once again pelleted at 500g for 3 min, and resuspended in hypotonic HEPES buffer (10 mM HEPES, pH

7.0; 5 mM 1,4-dithiothreitol (DTT); 2 mM Na-EDTA; 0.1% (w/v) CHAPS). After a 20 min incubation on ice, lysates were centrifuged at 10000g for 10 min. The supernatant was removed while taking care to avoid the pellet. Fifty microliter aliquots containing 2–4 μg of cytosolic protein (estimated by the Bradford method) were preincubated with 10 μM of appropriate protease inhibitor (benzyloxycarbonyl-Asp-Glu-Val-Asp-chloromethyl ketone and acetyl-Leu-Glu-His-Asp-chloromethyl ketone (both from Bachem, Heidelberg, FRG) for caspase 3 and 9, respectively) or DMSO (assay without inhibitor) for 5 min at 21 °C and then diluted to 198 μL with assay buffer (50 mM HEPES; 5 mM DTT; 2 mM Na-EDTA; 0.1% (w/v) CHAPS). The samples were frozen at -32 °C. All experiments were performed within 1 week of extract preparation.

Caspase 3 and 9 activities were assessed by monitoring cleavage of fluorochrome-tagged synthetic substrates Acetyl-Asp-Met-Gln-Asp-7-amino-4-methylcoumarin (Ac-DMQD-AMC) and Acetyl-Leu-Glu-His-Asp-amino-4-trifluoromethylcoumarin (Ac-LEHD-AFC) (both from Bachem), respectively, by HPLC. After the lysates were thawed, 2 μL of the appropriate substrate was added (final concentration of 150 and 200 μM for Ac-DMQD-AMC and Ac-LEHD-AFC, respectively). The samples were incubated for 30 min at 30 °C, and the specific products were quantified by RP-HPLC. The chromatography system used here consisted of an L-7100 pump controlled by a D-7000 interface (Merck, Darmstadt, Germany) and a 7125 Rheodyne sample injector fitted with a 20 μL injection loop. Detection was done with an L-7485 fluorescence detector (Merck); fluorescence was measured by using an excitation wavelength of 380 or 400 nm and an emission wavelength of 460 or 505 nm for released AMC or AFC, respectively.

Control experiments (data not shown) confirmed that the release of AMC or AFC was linear for at least 60 min at the conditions specified.

To estimate a specific caspase activity, measurements of blank (substrate only), negative control (substrate + cell lysate + inhibitor), and positive controls (substrate + cell lysate) were performed. From each result obtained as a fluorescence (peak area), a blank was subtracted. Standards containing 0–15 pmol of AMC and 0–30 pmol of AFC were utilized to determine the amount of fluorochrome released. The results are presented as the amount of AMC or AFC release ((pmol/mg)/min) that can be blocked by selective protease inhibitor.

HPLC Stability Studies. The HPLC system consisted of a P580 pump, a STH 585 column oven set at 37 °C, and a UVD 170S UV-vis detector, all from Dionex. Data management and analysis were done with the Chromleon software (Dionex). Injections were performed with a VICI microelectric valve actuator (Valco) fitted with a 500 μL injector loop. All chromatography was done with a 120-7 C18 Nucleosil column with a mobile phase of 3:2 MeOH/H₂O mM phosphate buffer (pH 3.3) at a flow rate of 0.6 mL/min. For all compounds, an amount of 500 μL of a 10 μM solution in buffer was injected and detection was done at the λ_{max} value. Thiourea dead-time was 3.6 min.

For stability determinations, the compounds were added to RPMI medium, medium + 10% FCS, or 5637 cells growing as described above for the cytotoxicity studies. A 1000-fold dilution from a DMF stock solution gave a final concentration of 10 μM. Samples were incubated in the dark at 37 °C in an atmosphere of 5% CO₂. At various time points, aliquots were removed and 500 μL were analyzed by HPLC. For samples containing FCS, ultrafiltration with an Amicon MPS system (Millipore) with a YMT 30 kDa filter was performed prior to chromatography.

Acknowledgment. Support from the Fonds der Chemischen Industrie (P.J.B.) and the European Community (P.R.) is acknowledged. P.R. also thanks the Sparkasse Vorpommern for financial support. We thank Prof. H.-H. Otto for valuable discussions.

Supporting Information Available: Tables 1S–14S of crystallographic data and elemental analysis data. This material is available free of charge via the Internet at <http://pubs.acs.org>.

References

- (1) Naruto, S.; Mizuta, H.; Yoshida, T.; Uno, H.; Kawashima, K.; Kadokawa, T.; Nishimura, H. Synthesis and spasmolytic activity of 2-substituted-3-(omega-dialkylaminoalkoxyphenyl)acrylonitriles and related compounds. *Chem. Pharm. Bull.* **1983**, *31*, 3022–2032.
- (2) Grundy, J. Artificial estrogens. F. Triphenylacrylonitrile and its analogs. *Chem. Rev.* **1957**, *57*, 357.
- (3) Kuzmierkiewicz, W.; Foks, H.; Baranowski, M. 3,5-Disubstituted derivatives of 1,2,4-triazole, synthesis and hypotensive activity. *Sci. Pharm.* **1985**, *53*, 133–138.
- (4) Parmar, V. S.; Kumar, A.; Prasad, A. K.; Singh, S. K.; Kumar, N.; Mukherjee, S.; Raj, H. G.; Goel, S.; Errington, W.; Puar, M. S. The synthesis of *E*- and *Z*-pyrazolylacrylonitriles and their evaluation as novel antioxidants. *Bioorg. Med. Chem.* **1988**, *25*, 911–914.
- (5) (a) Sawlewicz, J.; Milczarska, B.; Manowska, W. Reactions of cyanomethylbenzimidazoles. II. Reaction of cyanomethylbenzimidazoles with aldehydes, methylketones and nitroso compounds. *Pol. J. Pharmacol. Pharm.* **1975**, *27*, 187–201. (b) Kaliszan, R.; Milczarska, B.; Lega, B.; Szefer, P.; Janowiec, M. Studies on quantitative relationships between the structure and in vitro tuberculostatic potency of 2-cyanomethylbenzimidazole derivatives. *Pol. J. Pharmacol. Pharm.* **1978**, *30*, 585–91. (c) Sanna, P.; Carta, A.; Gherardini, L.; Rahbar Nikookar, Esmail, M. Synthesis and antimycobacterial activity of 3-aryl-, 3-cyclohexyl-, and 3-heteroaryl-substituted-2-(1*H*(2*H*)-benzotriazol-1(2-yl)prop-2-enitriles, prop-2-enamides and propenoic acids. II. *Farmaco* **2002**, *57*, 79–87.
- (6) Fujimoto, K.; Shimizu, M.; Takase, Y.; Nakanishi, I.; Nakamura, S. Relation between chemical structure and antimicrobial action of nitrofurans derivatives. IV. Antitrichomonal activity in vitro. *Chemotherapy (Tokyo)* **1967**, *15*, 535–541.
- (7) Shiba, S. A. Synthesis and insecticidal activity of novel acrylonitrile derivatives. *Phosphorus Sulfur* **1996**, *114*, 29–37.
- (8) Ohsumi, K.; Nakagawa, R.; Fukuda, Y.; Hatanaka, T.; Morinaga, Y.; Nihei, Y.; Ohishi, K.; Suga, Y.; Akiyama, Y.; Tsuji, T. Novel combretastatin analogues effective against murine solid tumors: design and structure–activity relationships. *J. Med. Chem.* **1998**, *41*, 3022–3032.
- (9) Brzozowski, Z.; Saczewski, F. Synthesis and antitumor activity of novel 2-amino-4-(3,5,5-trimethyl-2-pyrazolino)-1,3,5-triazine derivatives. *Eur. J. Med. Chem.* **2002**, *37*, 709–720.
- (10) Porousek, J. Preparation of 1-(2-benzimidazolyl)2-substituted ethylene derivatives by the Wittig reaction. *Collect. Czech. Chem. Commun.* **1991**, *56*, 1358–1360.
- (11) (a) Muir, J. A.; Cox, O.; Bernard, L. A.; Muir, M. M. Structure of 1-ethyl-2-(2'-chloro-4'-nitrostyryl)benzimidazole. *J. Crystallogr. Spectrosc. Res.* **1993**, *23*, 489–492. (b) Bacelo, D. E.; Cox, O.; Rivera, L. A.; Cordero, M.; Huang, S. D. (*E,Z*)-2-(2-Chloro-5-nitrostyryl)-1-(1-propenyl)benzimidazole. *Acta Crystallogr.* **1997**, *C53*, 907–909. (c) Perazza, M.; Rivera, L. A.; Cordero, M.; Huang, S. D. Crystal structure of (*E*)-2-(2-chloro-5-nitrostyryl)-1-(methylthio)methylbenzimidazole, C₁₇H₁₄ClN₃O₂S. *Z. Kristallogr. – New Cryst. Struct.* **1999**, *214*, 389–390. (d) Benakli, K.; Crozet, M. P.; Vanelle, P.; Giorgi, M. *Acta Crystallogr.* **1999**, *C55*, IUC9900041.
- (12) Dandarova, M.; Kovac, J.; Vegh, D.; Zvak, V. Furan derivatives. CLXIX. Stereochemistry of some substituted 2-furyl- and 2-thienyl ethylene derivatives. ¹H-NMR-study. *Collect. Czech. Chem. Commun.* **1982**, *47*, 3412–3417.
- (13) The structures of rotamers **11A–D** were fully optimized in the gas phase using the ab initio module (direct Hartree–Fock method, 6-31G** basis set) as implemented into the SPARTAN v 5.0 program installed on a Silicon Graphics O2 workstation.
- (14) Bodnar, A. G.; Ouellette, M.; Frolkis, M.; Holt, S. E.; Chiu, C.-P.; Morin, G. B.; Harley, C. B.; Shay, J. W.; Lichtsteiner, S.; Wright, W. E. Extension of life-span by introduction of telomerase into normal human cells. *Science* **1998**, *279*, 349–352.
- (15) Chang, H. Y.; Yang, X. Proteases for cell suicide: functions and regulation of caspases. *Microbiol. Mol. Biol. Rev.* **2000**, *64*, 821–846.
- (16) Martins, L. M.; Kottke, T.; Mesner, P. W.; Basi, G. S.; Sinha, S.; Frigon, N.; Tatar, E.; Tung, J. S.; Bryant, K.; Takahashi, A.; Svingen, P. A.; Madden, B. J.; McCormic, D. J.; Earnshaw, W. C.; Kaufmann, S. H. *J. Biol. Chem.* **1997**, *272*, 7421–7430.
- (17) Bednarski, P. J. Relationships between the aqueous chemistry and the in vitro cytotoxic activities of mixed-amine cisplatin analogues. *Biochem. Pharmacol.* **1992**, *43*, 2609–2620.
- (18) Gazit, A.; Oshero, N.; Gilon, C.; Levitzki, A. Tyrosinases. 6. Dimeric benzylidenemalonitrile tyrosinases: Potent inhibitors of EGF receptor tyrosine kinase in vitro. *J. Med. Chem.* **1996**, *39*, 4905–4911.
- (19) Friedman, M.; Cavins, J. F.; Wall, J. S. Relative nucleophilic reactivities of amino groups and mercaptide ions in addition reactions with α,β -unsaturated compounds. *J. Am. Chem. Soc.* **1965**, *87*, 3672–3682.
- (20) (a) Campian, E. C.; Cai, J.; Benz, F. W. Acrylonitrile irreversibly inactivates glyceraldehyde-3-phosphate dehydrogenase by alkylating the catalytically active cysteine 149. *Chem.-Biol. Interact.* **2002**, *140*, 279–291. (b) Langvardt, P. Acrylonitrile. In *Ullmann's Encyclopedia of Industrial Chemistry*; VCH: Weinheim, Germany, 1985; Vol. A1, pp 177–184.
- (21) Buchter, A.; Peter, H.; Bolt, H. M. *N*-Acetylcysteine as an antidote in accidental acrylonitrile poisoning. *Int. Arch. Occup. Environ. Health* **1984**, *53*, 311–319.
- (22) (a) Benz, F. W.; Nerland, D. E.; Corbett, D.; Li, J. Biological markers of acute acrylonitrile intoxication in rats as a function of dose and time. *Fundam. Appl. Toxicol.* **1997**, *36*, 141–148. (b) Benz, F. W.; Nerland, D. E.; Li, J.; Corbett, D. Dose dependence of covalent binding of acrylonitrile to tissue protein and globin in rats. *Fundam. Appl. Toxicol.* **1997**, *36*, 149–156.
- (23) Browne, E. J.; Polya, J. B. Triazoles. Part VII. Syntheses of substituted 1,2,4-triazoles. *J. Chem. Soc.* **1962**, 5149–5152.
- (24) Copeland, R. A. B.; Day, A. R. The preparation and reactions of 2-benzimidazolecarboxylic acid and 2-benzimidazoleacetic acid. *J. Am. Chem. Soc.* **1943**, *65*, 1072–1075.
- (25) Shiba, S. A. Decomposition of 2-propenyl azide derivatives. Synthesis and larvicidal activity of novel products. *Arch. Pharm.* **1998**, *331*, 91–96.
- (26) Rao, P. Shanthan, Venkataratnam, R. V. Anhydrous zinc chloride catalysis in carbonyl-methylene condensations: synthesis of arylideneacetone nitriles and arylidene heterocycles. *Indian J. Chem., Sect. B* **1993**, *32*, 484–486.

JM0311036